Predicting Synchrony in Heterogeneous Pulse Coupled Oscillators

Sachin S. Talathi[1],* Dong-Uk Hwang[1], Abraham Miliotis[1], Paul R. Carney[1], and William L. Ditto[1]

[1] J Crayton Pruitt Department of Biomedical Engineering,
University of Florida, Gainesville, FL 32611

Pulse coupled oscillators (PCO's) represent an ubiquitous model for a number of physical and biological systems. Phase response curves (PRC's) provide a general mathematical framework to analyze patterns of synchrony generated within these models . A general theoretical approach to account for the nonlinear contributions from higher order PRC's in the generation of synchronous patterns by the PCO's is still lacking. Here, by considering a prototypical example of a PCO network, i.e., two synaptically coupled neurons, we present a general theory that extends beyond the weak coupling approximation, to account for higher order PRC corrections in the derivation of an approximate discrete map, the stable fixed point of which can predict the domain of 1:1 phase locked synchronous states generated by the PCO network.

Networks of pulse-coupled oscillators (PCO's) are used in the study of a wide range of physical and biological systems such as the plate tectonics in earthquakes, pacemaker cells in the heart, flashing flies and the neurons in the brain [1–3]. These systems interact by transmitting and receiving discrete time pulses that interfere the otherwise smooth time evolution of the oscillator [4]. The emergence of synchrony is a ubiquitous collective dynamical feature observed in these networks [5–7]. The mathematical technique of phase reduction is commonly employed in the study of the patterns of synchrony generated by these networks [8]. The technique involves determining the phase response curve (PRC) for an oscillator that quantifies how the oscillator shifts in phase in response to a perturbation through a pulsatile input. Given the PRC, one can construct a discrete map that can be used to predict the entrainment of an oscillator to a periodic stimulus and phase locking in a network of PCO's [9]. In most physical systems modeled as PCO networks, the infinitesimal phase response curve (iPRC), which represents the oscillators response to a weak perturbation, suffices to understand the collective dynamical properties such as synchrony, wave propagation and pattern generation in these oscillator networks [10, 11]. However when the oscillators are interacting through a strong coupling, the weak coupling limit may give wrong results [12, 13]. This is because the large deviations from the limit cycle caused by strong coupling may persist into at least one cycle beyond the cycle containing the perturbation [14, 15]. In these cases, higher order PRC terms are non zero and play a significant role in determining the stability of synchrony generated by the PCO network.

To our knowledge, a general theoretical approach to account for the non-linear effects of higher order PRC terms in the synchrony of a PCO network is still lack-

ing. Here we present a general mathematical framework that allows us to incorporate the nonlinear contributions from higher order PRC terms in the approximation of a discrete map that is used to predict the stability of 1:1 synchrony in a PCO network. We consider a prototypical example of a PCO network, i.e., two synaptically coupled interneurons, to develop our theory. The choice of the synaptically coupled interneurons in this study is motivated by the importance of inhibitory neuronal networks in the generation of synchronous brain rhythms, which are known to constitute a fundamental mechanism for information processing in the brain [16, 17]

Each oscillator in the PCO network considered here is represented by a single compartment conductance based fast spiking interneuron model [18]. The dynamical equation for the model neuron is given by

$$
\begin{aligned}
C\frac{dV(t)}{dt} &= I_{DC} + I_S(t) + g_{Na}m_\infty^3 h(t)(E_{Na} - V(t)) \\
&+ g_K n^4(t)(E_K - V(t)) + g_L(E_L - V(t)) \quad (1)
\end{aligned}
$$

where V(t) is the membrane potential, I_{DC} is the constant input DC-current that determines the intrinsic spiking period T_0, E_r and g_r represent the reversal potential and conductance of ion channels with parameters obtained from [18]. The gate variables m_∞, $h(t)$ and $n(t)$ satisfy first order kinetic equations decribed in [18]. The resting potential of neuron is $V_{\text{rest}} = -65$ mV ($I_{DC} = 0$) and the threshold for the generation of an action potential is $V_T \approx -55$ mV. $I_S(t) = g_s S(t)(E_R - V(t))$ is the synaptic current (E_R: reversal potential in mV; g_s: synaptic conductance in mS/cm^2). $S(t)$ satisfies a first order kinetic equation as described in [19–21].

The PRC for a neuron receiving perturbation through a synapse is in general a function of the synaptic parameters and depending on the strength of synaptic input, the perturbations can have strong effect on the period of neuronal spiking. As a result in this case

---

*Electronic address: sachin.talathi@bme.ufl.edu

the PRC is measured in terms of time rather than phase of perturbing input and is referred to as the spike time response curve (STRC) [22]. STRC's provide a natural experimental framework to study the perturbation effects of synapses on the firing times of a neuron without the requirement of a model to mimic neuronal dynamics. Following Acker et.al. [22], we define the STRC's for a neuron oscillator as: $\Phi_j(\delta t, \tau_R, \tau_D, g_s, E_R, T_0) = \frac{T_j - T_0}{T_0}$ where T_0 is the intrinsic period of spiking, T_j represents the length of the jth spiking cycle from the cycle $j = 1$ in which the neuron receives synaptic stimuli at time $0 < \delta t < T_0$. The synaptic parameters are: τ_R: the synapse rise time, τ_D: the synaptic decay time, g_s: the synaptic strength and E_R: the reversal potential of the synapse. In general the synaptic input need not be weak [23, 24]. We have assumed that the intrinsic period of spiking for the neuron T_0, is constant in our definition of STRC above. We therefore exclude the important case of a neuron exhibiting spike frequency adaptation [25]. Recent work by [26] addresses the issue of spike frequency adaptation using functional phase response curves which are generated using a train of pulses applied at a fixed delay after each spike, with the PRC measured when the phasic relationship between the stimulus and the subsequent spike in the neuron has converged. The STRC's are obtained numerically [22] as explained through Figure 1a. The neuron firing regularly with period T_0, is perturbed through an inhibitory synapse at time δt after the neuron has fired a spike at reference time zero. The spiking time for neuron is considered to be the time when the membrane voltage V, crosses a threshold (set to 0 mV in all the calculations presented here). As a result of this perturbation, the neuron fires the next spike at time t_1, representing the first cycle after perturbation of length $T_1 \neq T_0$. Depending on the properties of the synapse, i.e., g_s, τ_R, τ_D and E_R; the length of subsequent cycles might change. In Figures 1b and 1c, we show STRC's calculated for a neuron receiving synaptic input from a hyperpolarizing ($E_R < V_{rest}$) and a shunting ($V_{rest} < E_R \leq V_T$) synapse respectively. For hyperpolarizing inhibition the first order STRC is non-zero for all perturbation times $0 < \delta t < T_0$; the second order STRC is non-zero for $\delta t \to T_0$ and all higher order STRC terms are zero. However for shunting inhibition the effect of perturbation lasts for the first three cycles including the perturbing cycle, i.e., both the first order and second order STRC's are non-zero for $0 < \delta t < T_0$ and the third order STRC is non-zero for $\delta t \to T_0$. Higher order STRC terms for shunting synapse are present because, strong shunting input tends to depolarize the neuron towards the threshold for spiking thereby reducing the effective time for the occurrence of the next spike. For all further calculations, unless otherwise mentioned, we will suppress the dependence of STRC on synaptic parameter's and the intrinsic period of the neuron T_0. We further define the following two functions derived from STRC's: The recovery time following a single synaptic perturbation

$R(\delta t) = T_0 (1 + \Phi_1(\delta t)) - \delta t$ and the period of jth firing cycle, $E_j(\delta t) = T_0(1 + \Phi_j(\delta t))$ ($j = 1$, corresponds to the firing cycle in which the neuron receives its synaptic perturbation).

We will now use STRC's to present a general theoretical approach to determine an approximate discrete map for 1:1 synchrony between two synaptically coupled interneurons. We will consider the specific example of shunting inhibition to formulate our theory because of the significant non-zero contributions from the higher order PRC terms. Shunting inhibition in networks of interneurons have also recently been demonstrated to play an important role in the generation of synchronous gamma rhythms in the brain [24]. We begin by considering the simple case of a periodically firing neuron that receives synaptic stimuli through a shunting synapse in each of its two successive firing cycles at times δt_1 and δt_2 as shown in Figure 2. Our goal is to determine the length of the second cycle T_2.

In the presence of a single perturbation at δt_1 in the cycle 1, following from the definition of STRC's we have $T_2 = E_2(\delta t_1) = T_0(1 + \Phi_2(\delta t_1))$. Similarly in the presence of a single perturbation in cycle 2 at time δt_2, again following from the definition of STRC's we have $T_2 = \delta t_2 + R(\delta t_2) = T_0(1 + \Phi_1(\delta t_2))$. In writing this equation we made an implicit assumption that the default period of second cycle in the absence of the single perturbation at time δt_2 is T_0. However if the synaptic input at δt_2 is preceded by a synaptic perturbation in the previous cycle at δt_1, the default length of the second cycle is no longer T_0. Therefore, in order to correctly determine the length of second cycle in this case, we have to compensate for the change in the default length of second cycle caused by synaptic input at time δt_1. This compensation is done by re-normalizing the synaptic perturbation time in the second cycle to $\delta t_2^e = \delta t_2 \frac{T_0}{E_2(\delta t_1)}$ and re-scaling the phase of the trajectory at the time of second perturbation by $\alpha_2^e = \frac{\delta t_2}{E_2(\delta t_1)} - \frac{\delta t_2}{T_0}$ as explained through schematic diagram in Figure 2.

In Figure 2 we provide a detailed schematic of various changes in spike times resulting from two consecutive synaptic perturbations to provide an intuitive idea behind our proposed re-normalization and re-scaling procedure. We assume that the drift away from the limit cycle resulting from synaptic perturbations at times δt_1 and δt_2 can be represented by a change in the phase velocity of the resulting trajectory rather than the perturbation of the trajectory away from the limit cycle. Our assumption as stated about implies that the firing frequency of the resulting trajectory is modified such that the new intrinsic period of firing of the oscillator is $E_2(\delta t_1)$. Since the open loop STRC defined above is dependent on the intrinsic period of the oscillator, the change in the firing period of the oscillator from T_0 to $E_2(\delta t_1)$, will change the shape of the open loop STRC

function. We assume that this change is linear in that (a) the STRC will either stretch ($E_2(\delta t_1) > T_0$) or shrink ($E_2(\delta t_1 < T_0$) along the perturbation time axis. The application of the similarity triangles property to the phase plot described in Figure 2 allows us to compensate for change in the shape of STRC by re-normalizing the effective time of synaptic perturbation to δt_e^2. The change in phase velocity of the trajectory also means that the neuron now receives different amount of net current for a given magnitude of synaptic perturbation. In order to account for the true effect of synaptic perturbation on the original trajectory, we also have to rescale the effective phase of the synaptic perturbation. Again going back to schematic diagram in Figure 2, this compensation is done by modifying the effective phase of synaptic perturbation to α_2^e. In order to determine how the effective phase modifies the effective recovery time of the trajectory, we empirically fit the modified recovery period to the rescaled phase of the synaptic perturbation. The best fit in the least squares sense was obtained by rescaling the effective recovery period to $R(\delta t_2^e)(1 - \alpha_2^e)$.

The length of cycle 2 can now be written as $T_2 = \delta t_2 + R(\delta t_2^e).(1 - \alpha_2^e)$. In terms of STRC's we have,

$$T_2 = \delta t_2 + \left(T_0 \left(1 + \Phi_1 \left(\frac{\delta t_2}{1 + \Phi_2(\delta t_1)} \right) \right) - \frac{\delta t_2}{1 + \Phi_2(\delta t_1)} \right)$$
$$\times \left(1 - \frac{\delta t_2}{T_0(1 + \Phi_2(\delta t_1))} + \frac{\delta t_2}{T_0} \right) \quad (2)$$

When $\Phi_2(x) \approx 0$ (see Figure 1b) eq.1 reduces to

$$T_2 \approx T_0(1 + \Phi_1(\delta t_2) + \Phi_2(\delta t_1)) \quad (3)$$

The approximation in the form of eq. 3 has been derived earlier by [12, 13, 27] to analyze the effect of periodic perturbation on a periodically firing neuron under the assumption that the second order resetting is complete and the trajectory returns to its limit cycle before the arrival of subsequent perturbation. In other words the resetting by the synaptic perturbation was assumed to be instantaneous. This is most likely the situation for hyperpolarizing synaptic input for which $\Phi_2(\delta t) \approx 0$ unless $\delta t \to T_0$. The authors have successfully used this approximation to demonstrate effect of second order STRC component on stability of 1:1 synchronous state in a ring of pulse coupled oscillators [12]; to determine phase resetting and phase locking in a hybrid circuit of one model neuron and one biological neuron [13]; and more recently to predict 1:1 and 2:2 synchrony in mutually coupled network of interneurons with synapse that is hyperpolarizing [27]. As stated above, we do not assume instantaneous resetting and we do not consider the situation when the neuron receives periodic perturbation. Instead, the effect of synaptic perturbation is considered to change the phase velocity of the trajectory on the limit cycle and we determine the effective length of second firing cycle in the presence of two consecutive synaptic perturbations.

The ability for eqs.2 and 3 to successfully predict the length of second cycle is quantified by determining the percent error $\delta E_2(\delta t_1, \delta t_2) = 100 \left| \frac{T_2^N - T_2^P}{T_2^N} \right|$ between the predicted value for the length of second cycle: T_2^P and the actual value: T_2^N, determined by numerically solving the ODE in eq.1. In Figure 3 and , we plot the color coded percent error $\delta E_2(\delta t_1, \delta t_2)$ for a neuron receiving stimuli through a shunting synapse with parameters: $g_s = 0.15$ mS/cm^2, $\tau_R = 0.1$ ms, $\tau_D = 8$ ms, and $E_R = -55$ mV. The inset shows the plot of T_2^N and T_2^P for the specific case of $\delta t_1 = 15$ ms. We see that while eq.2 is correctly able to predict the length of second cycle (Figure 3a), eq.3 *fails* to capture the effect of second order STRC contribution in determining T_2 (Figure 3b). We would like to emphasize that the expression for the predicted value of T_2 through eq.2 is only dependent on STRC's estimated for a given synapse type without any explicit assumption on the strength of synaptic input to the neuron and is valid *both* in the regime of weak and strong coupling and for slow and fast synaptic dynamics.

We now generalize our approach of re-normalization and re-scaling to consider the situation when the neuron receives 3 synaptic stimuli in 3 consecutive firing cycles at time δt_1 in cycle 1, at time δt_2 in cycle 2 and at time δt_3 in cycle 3. This is an important case to consider since we know from Figure 1c that the effect of a perturbation through a shunting synapse last for 3 consecutive firing cycles of the neuron. We first determine the length of third cycle $\tilde{E}_3(\delta t_1, \delta t_2)$, when the neuron receives two synaptic stimuli at times δt_1 and δt_2. Since $\Phi_3(\delta t) \approx 0$ (see Figure 1c), following eq.3 we can approximate $\tilde{E}_3 \approx T_0 (1 + \Phi_2(\delta t_2^e) + \Phi_3(\delta t_1))$. Now, following from eq.2, the length of 3rd cycle in the presence of three consecutive synaptic stimuli can be written as: $T_3 \approx \delta t_3 + R(\delta t_3^e).(1 - \alpha_3^e) + T_0\Phi_3(\delta t_1)$; where $\delta t_3^e = \delta t_3 \frac{T_0}{\tilde{E}_3(\delta t_1, \delta t_2)}$ and $\alpha_3^e = \frac{\delta t_3}{\tilde{E}_3(\delta t_1, \delta t_2)} - \frac{\delta t_3}{T_0}$. Note the addition of the term $T_0\Phi_3(\delta t_1)$, which determines the contribution of the first spike to the third cycle.

We can now derive the approximate discrete map for 1:1 synchrony between neurons A and B firing with intrinsic period $T_0^A \neq T_0^B$ and coupled through a shunting synapse (see Figure 4a). The heterogeneity in the intrinsic firing rates of the two coupled neurons is quantified through $H = 100 \cdot \frac{I_{DC}^B - I_{DC}^A}{I_{DC}^A}$, where I_{DC}^A and I_{DC}^B are constant DC currents driving neurons A and B. From Figure 4a, when the two neurons are locked in stable 1:1 synchrony we have for neuron A, $t_{n+1}^A \approx t_n^A + \delta_n + R \left(\delta_n \frac{T_0^A}{\tilde{E}_3(\delta_{n-2}, \delta_{n-1})} \right).(1 - \alpha_3^e) + T_0^A\Phi_3(\delta_{n-2})$, where t_n^X is the time of n$^{\text{th}}$ spike for neuron X={A,B} and $\delta_n = \delta t_n^B - \delta t_n^A$. Since neuron B, does not receive any external perturbation, we have for neuron B, $t_{n+1}^B = t_n^B + T_0^B$. The discrete map for the evolution of

δ_n can then be obtained as:

$$\delta_{n+1} \approx T_0^B - R\left(\delta_n \frac{T_0^A}{\tilde{E}_3(\delta_{n-2}, \delta_{n-1})}\right).(1 - \alpha_3^e)$$
$$- T_0^A \Phi_3(\delta_{n-2}) \qquad (4)$$

The steady state solution to above equation can be obtained by solving for the fixed point δ^* defined by $\delta_{n+1} = \delta_n = \delta_{n-1} = \delta_{n-2} = \delta^*$. We then obtain $F(\delta^*) = T_0^B$, where $F(\delta^*)$ is given by

$$F(\delta^*) \approx \delta^* + T_0^A \Phi_3(\delta^*) + R\left(\frac{\delta^* T_0^A}{\tilde{E}_3(\delta^*, \delta^*)}\right)$$
$$\times \left(1 - \frac{\delta^*}{\tilde{E}_3(\delta^*, \delta^*)} + \frac{\delta^*}{T_0^A}\right) \qquad (5)$$

In the limit of $\Phi_2 \approx 0$ and $\Phi_3 = 0$, $F(\delta^*) \approx T_0^A(1 + \Phi_1(\delta^*) + \Phi_2(\delta^*))$ corresponding to the well-known equation for the solution to the fixed point of discrete map for synchrony between coupled oscillators with any type of pulsatile coupling with no higher order PRC contributions [20]. Stability of the fixed point δ^* representing the solution to eq.5 requires $0 < \left|\frac{\partial F(\delta_n, \delta_{n-1}, \delta_{n-2})}{\partial(\delta_n, \delta_{n-1}, \delta_{n-2})}\right|_{\delta_n = \delta_{n-1} = \delta_{n-2} = \delta^*} < 2$. This stable fixed point represents the 1:1 phase locked state for the two coupled interneurons.

In order to determine whether eq.4 can predict 1:1 phase locked states for the two pulse coupled neurons considered above, we apply the discrete map to the specific case of neurons A and B coupled through a shunting synapse with parameters: $E_R = -55$ mV, $\tau_R = 0.1$ ms, and $\tau_D = 8$ ms. Neuron A receives fixed dc current I_{DC}^A, such that it is firing with intrinsic period of $T_0^A = 31$ ms. We solve eq.5, for different values of H, thereby modulating T_0^B, to determine the set of values for g_s, which will result in stable fixed point solution for eq.5. The solution is obtained by estimating STRC's for each value of g_s and then determining whether there is a fixed point solution to eq.5. In Figure 4c, we present the results of this calculation. For a given value of H, the curve in black gives the lower and upper bounds on the strength of coupling for shunting synapse g_s, for which a unique stable solution to eq.5 exists. For example with H=50, the range of values for g_s for which a unique stable solution exists for eq.5 is $0.09 < g_s < 0.21$. This region of 1:1 synchronous locking is analogous to the classic Arnold tongue [20, 28], obtained for synchrony between two coupled nonlinear oscillators. In Figure 4b, the general feature of the Arnold tongue is represented as the region bounded by two black curves obtained through STRC by solving for fixed point of eq.5. In Figure 4b, shown in blue is a similar bound on the range of heterogeneity leading to synchronous oscillations between the two coupled neurons, obtained by numerically solving eq.1 for the evolution of the

dynamics of the two synaptically coupled neurons. This curve is obtained by fixing the firing period of neuron A, T_0^A and varying the firing period of neuron B, by changing I_{DC}^B and determining the strength of synaptic coupling g_s that results in $\frac{T_0^B}{\langle T^A \rangle} \approx 1$. As can be seen from Figure 4b, the results match to those obtained through STRC calculations for fixed point of eq.5.

Similar analysis can be performed to derive an approximate discrete map for 1:1 synchrony between neurons A and B when they are mutually coupled to each other as shown in Figure 4c (inset). The discrete map for the evolution of δ_n in this case is given as:

$$\delta_{n+1} \approx R^B\left(\delta_n' \frac{T_0^B}{\tilde{E}_3^B(\delta_{n-2}', \delta_{n-1}')}\right).(1 - \alpha_3^{eB})$$
$$+ T_0^B \Phi_3^B(\delta_{n-2}') \qquad (6)$$

where $\delta_n' = t_{n+1}^A - t_n^B$ (see Figure 4a) and is given as:

$$\delta_n' \approx R^A\left(\delta_n \frac{T_0^A}{\tilde{E}_3^A(\delta_{n-2}, \delta_{n-1})}\right).(1 - \alpha_3^{eA})$$
$$+ T_0^A \Phi_3^A(\delta_{n-2}) \qquad (7)$$

The function's R^X and α_3^{eX}, $X = \{A, B\}$ are given through STRC estimates obtained for neuron's A and B which are dependent on their intrinsic firing rates T_0^A and T_0^B respectively. Numerically estimated Arnold Tongue and the analytically estimated Arnold tongue for the case of $E_R = -60$ mV, $\tau_D = 2$ ms, is shown in Figure 4c.

In conclusion, by considering the specific example of a PCO network, i.e., synaptically coupled neurons, we have provided a general theoretical approach of re-scaling and re-normalization to account for the non-linear contributions from the higher order PRC's in the approximation of a discrete map that can be used to predict the stability of 1:1 synchronous state in heterogeneous pulse coupled oscillators. The methodology presented here provides a general (beyond the limit of weak coupling) model independent framework to predict the emergence of synchrony within a heterogeneously coupled PCO network. We conclude by noting that the methodology presented here cannot be directly applied to predict patterns of synchrony in a larger network of PCO's, however the ability to predict local synchrony between pairs of heterogeneously coupled PCO's may provide clues for observing synchrony in a large network of PCO's.

postdoctoral fellowship.

[1] Z. Olami, J. Feder, and K. Christensen, Phys Rev Lett **68**, 1244 (1992).
[2] J. Buck and E. Buck, Scientific American **234**, 74 (1976).
[3] J. Jalife, J Physiol **356**, 221 (1984).
[4] C. Kirst and M. Timme, arXiv.org **0812.1786v1** (2008).
[5] R. Mirollo and S. Strogatz, SIAM J. Appl Math **50**, 1645 (1990).
[6] U. Ernst, K. Pawelzik, and T. Geisel, Phys Rev Lett **74**, 1570 (1995).
[7] P. Bressloff, S. Coombes, and B. de Souza, Phys Rev Lett **79**, 2791 (1997).
[8] A. Winfree, *The geometry of biological time* (Springer Verlag NY, 2001), 2nd ed.
[9] J. Murray, *Mathematical Biology* (Springer Verlag Berlin, 1993).
[10] A. Preyer and R. Butera, Phys Rev Lett **95**, 138103 (2005).
[11] R. Galan, G. Ermentrout, and N. Urban, Phys Rev Lett **94**, 158101 (2005).
[12] S. Oprisan and C. Canavier, Differential Equations and Dynamical Systems **9**, 243 (2001).
[13] S. Oprisan, A. Prinz, and C. Canavier, Biophysical J **87**, 2283 (2004).
[14] M. Guevara, A. Shrier, and L. Glass, Heart Circ. Physiol. **20**, H1298 (1986).
[15] C. Canavier, Scholarpedia **1**, 1332 (2006).
[16] A. Engel and W. Singer, TRENDS in Cog Sci **5**, 16 (2001).
[17] T. Mima, T. Oluwatimilehin, T. Hiraoka, and M. Hallett, J Neurosci **21**, 3942 (2001).
[18] X. Wang and G. Buzsaki, J Neurosci **16**, 6402 (1996).
[19] H. Abarbanel and S. Talathi, Phys Rev Lett **96**, 148104 (2006).
[20] S. Talathi, D. Hwang, and W. Ditto, J Comp Neurosci **25**, 262 (2008).
[21] S. Talathi, H. Abarbanel, and W. Ditto, Phys Rev E **78**, 031918 (2008).
[22] C. Acker, N. Kopell, and J. White, J Comp Neurosci **15**, 71 (2004).
[23] B. Ermentrout and N. Kopell, SIAM J. Appl Math **50**, 125 (1990).
[24] M. Bartos, I. Vida, and P. Jonas, Nature Rev Neurosci **8**, 45 (2007).
[25] S. Crook, G. Ermentrout, and B. JM., Neural Compute **10**, 837 (1998).
[26] J. Cui, C. Canavier, and R. Butera, J Neurophysiol **Epub ahead of print** (2009).
[27] S. Maran and C. Canavier, J Comp Neurosci **24**, 37 (2008).
[28] J. Kurths, A. Pikovsky, and M. Rosenblum, *Synchronization, a universal concept in non-linear science* (Cambridge University Press, 2001).
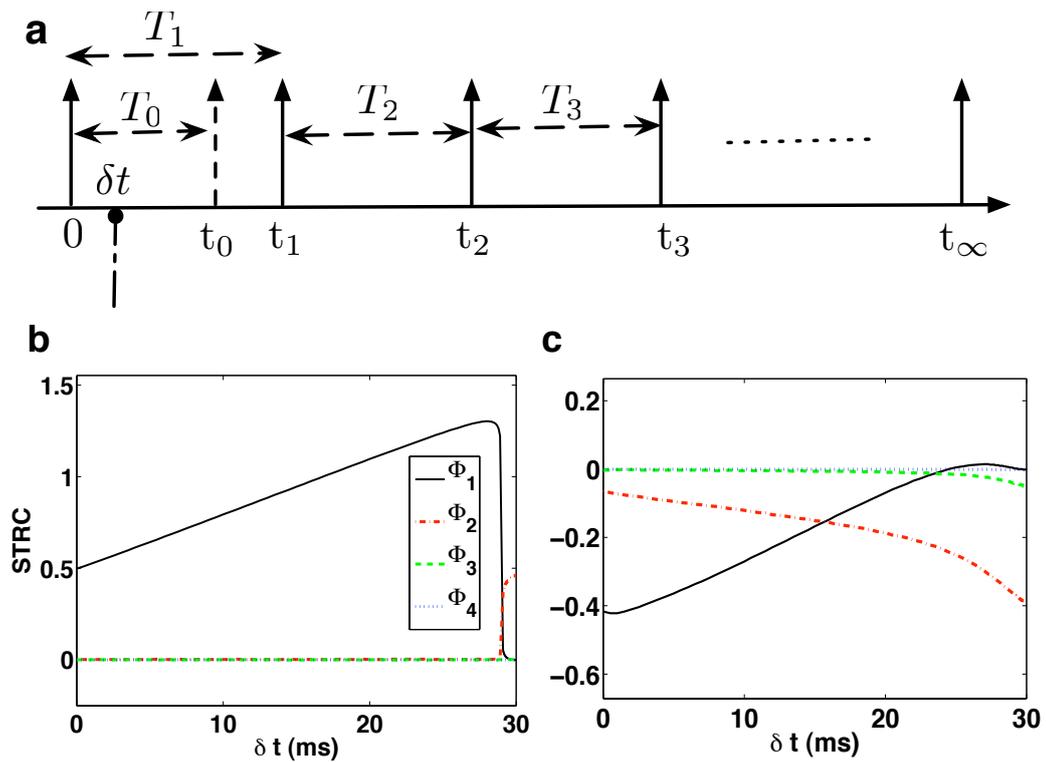
Figure 1: (Color Online) (a) Schematic diagram demonstrating the effect of perturbation received by a spiking neuron at time δt. The cycle containing the perturbation defines the first order STRC and the subsequent cycles define the higher order STRC terms. (b) The STRC's Φ_1 (black line), Φ_2 (red dash-dot line), Φ_3 (green dashed line), Φ_4 (blue dotted line), for hyperpolarizing synaptic input with $E_R = -75$ mV. (c) The STRC's for shunting synaptic input with $E_R = -55$ mV. The synaptic parameters are $\tau_R = 0.1$ ms, $\tau_D = 8$ ms, $g_s = 0.15$ mS/cm^2 . The intrinsic period of firing for the neuron is $T_0 = 31$ ms and $V_{\text{rest}} = -65$ mV.
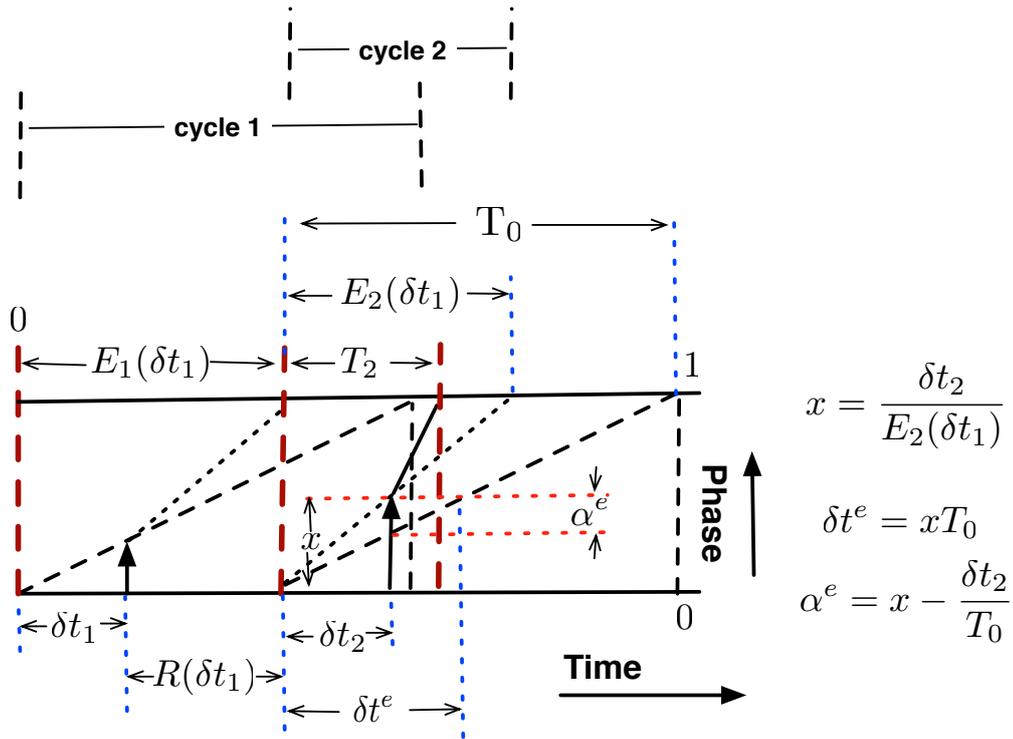
Figure 2: (Color Online) Schematic diagram to demonstrate the re-normalization and re-scaling procedure to determine the length of second cycle T_2. Red dashed (dark gray) lines represent the effective spike times after the neuron receives two consecutive synaptic perturbations. Black dotted lines represent the chage in the firing cycle caused by synaptic input in the first firing cycle. Shown in black dashed line is the unperturbed firing cycle for the neuron. We assume that the drift away from the limit cycle caused by the synaptic perturbations (at times δt_1 and δt_2) can be represented through the change in the phase velocity of the trajectory. This assumption allows us to use similarity of triangle properties to determine the re-normalized stimulus time δt^e and the re-scaled phase of the trajectory at the instance of second synaptic perturbation given by α^e.
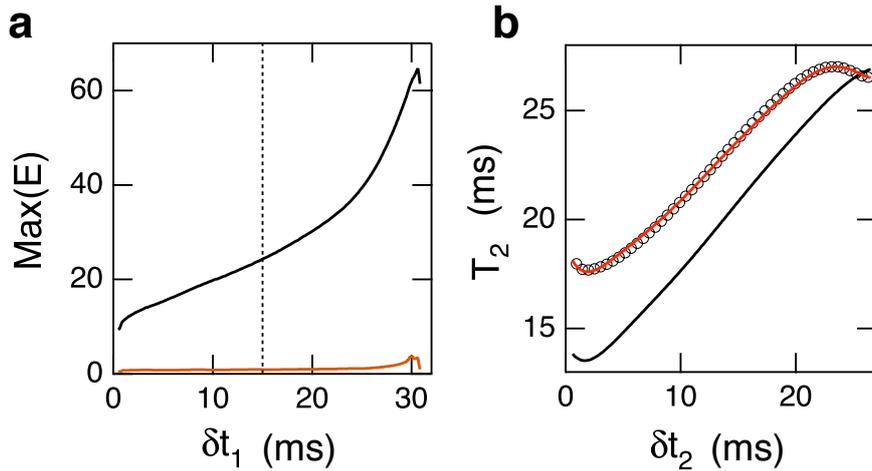

Figure 3: (Color Online) (a) Maximum error between the predicted value T_2^P determined from eq. 2 (red, "light gray") and eq.3 (black) respectively and the numerically estimated value T_2^N. (b) T_2 as function of δt_2 determined using eq. 2 (red, "light gray"), eq. 3 (black) and through numerical simulations (open black circles) for $\delta t_1 = 15$ ms.
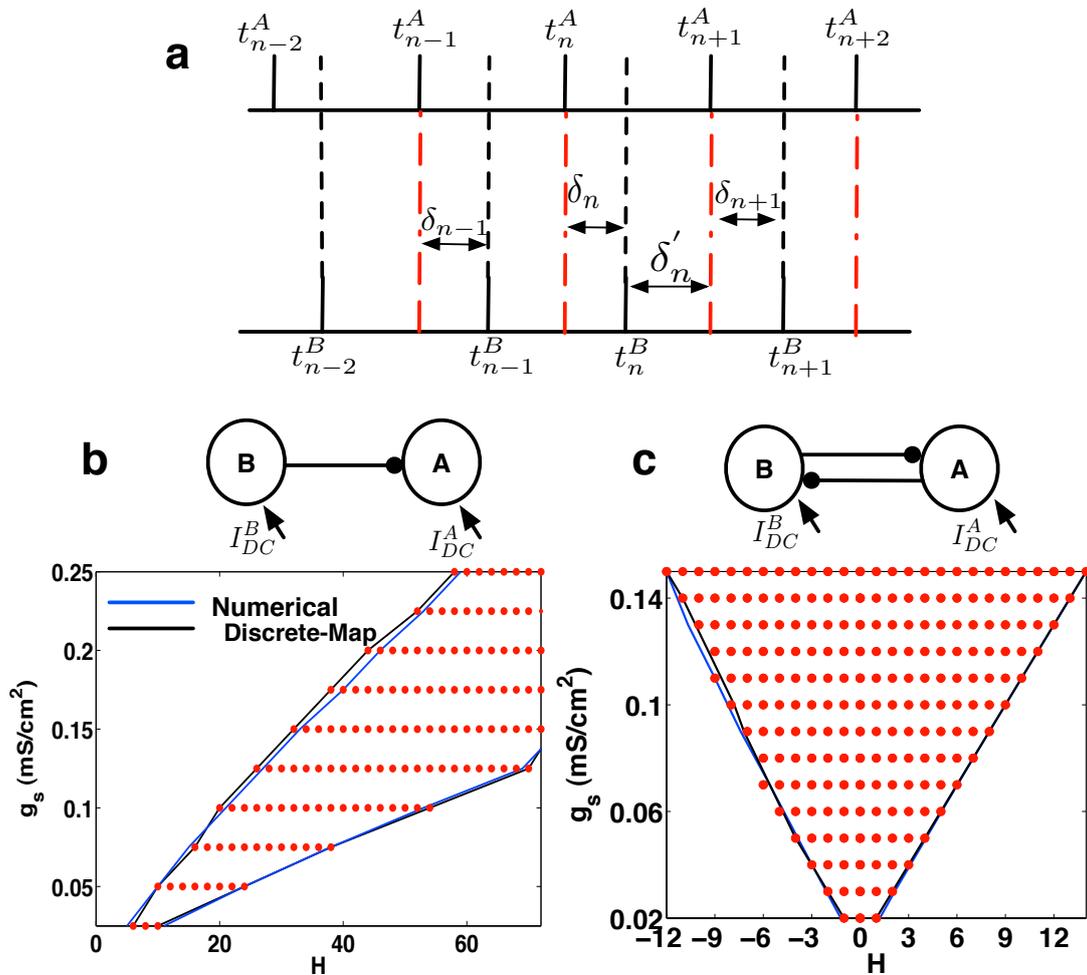
Figure 4: (Color Online) (a) Schematic diagram representing spike timing for neurons A and B when they are phase locked in 1:1 synchrony. (b) we show domain of 1:1 synchrony estimated through STRC's from the discrete map in eq.5 (shown in black) and those obtained through numerical simulations of the network (shown in blue, "dark gray") for two unidirectionally coupled interneurons coupled with shunting synapse with parameters $\tau_R = 0.1$ ms, $E_R = -55$mV and $\tau_D = 8$ ms. The pair of g_S-H values for which we solve the discrete map in eq. 4 to determine the stable fixed point for 1:1 synchrony is shown in red filled circles within the Arnold's tongue. (c) The domain of 1:1 synchrony estimated through the discrete map from eq's 6 and 7 (shown in black) and those obtained through numerically simulations for mutually coupled interneurons as shown in the inset with synaptic parameters $\tau_R = 0.1$ ms, $E_R = -60$mV and $\tau_D = 2$ ms. The pair of g_S-H values for which we solve the discrete map in eq. 6-eq.7 to determine the stable fixed point for 1:1 synchrony is shown in red filled circles within the Arnold's tongue.